INTERNATIONAL JOURNAL OF CLIMATOLOGY
Int. J. Climatol. **30**: 582–600 (2010)
Published online 3 April 2009 in Wiley InterScience
(www.interscience.wiley.com) DOI: 10.1002/joc.1908

RMetS
Royal Meteorological Society

Twice wind onsets of monsoon over the western North Pacific and their simulations in AMIP models

Li Zhang[a,b] and Jianping Li[a]*

[a] *State Key Laboratory of Numerical Modeling for Atmospheric Sciences and Geophysical Fluid Dynamics, Institute of Atmosphere Physics, Chinese Academy of Sciences, Beijing 100029*

[b] *Graduate University of Chinese Academy of Sciences, Beijing 100049*

ABSTRACT: The absolute angle between wind vectors is used to investigate and describe the seasonal evolutions of wind direction, which is able to indicate the abrupt seasonal shift and stable seasonal state of winds. The results show that the wind directions over the western North Pacific (WNP, 10°–22.5°N, 125°–145°E) undergo two abrupt changes and three stable states from winter to summer. Here we name the phenomenon as twice wind onsets of monsoon. The first wind onset occurs near mid-May at 15°N, and the second one happens with the wind direction shifting southwesterly in mid-July and ends in late September. The variations of Outgoing Longwave Radiation (OLR) and rainfall in the northward 5° latitudes of the neighbouring region show similar abrupt features as those of the twice wind onsets. The western Pacific subtropical high (WPSH) retreats eastward in the second stable state (pentad 29 to 37), which differs from the first stable state (pentad 1 to 24). As the strong cross-equator flows from the Southern Hemisphere reach the WNP, the eastward retreat of WPSH consequently triggers the first wind onset. Then the WPSH ridge suddenly jumps to 30°N and results in the second wind onset. Meanwhile, the propagation of the second wind onset is consistent with the migration of the WNP monsoon trough.

Seven atmospheric general circulation models (AGCMs) of Atmospheric Model Intercomparison Project (AMIP) from Intergovernmental Panel on Climate Change (IPCC) Fourth Assessment Report (AR4) are validated against the observations mentioned earlier. The results show that there are still notable shortcomings for the models to simulate the WNP summer monsoon, especially the twice onsets. There is no significant improvement for the simulation of multi-models ensemble mean. Only MPI-ECHAM5 captures partial characteristics of similar pattern. The poor simulation of the migration of the WPSH ridge and monsoon trough may be important factors for the shortcomings. Moreover, none of the models reproduces corresponding rainfall patterns over the WNP. Copyright © 2009 Royal Meteorological Society

KEY WORDS monsoon; twice wind onsets; western North Pacific; AMIP models

Received 30 April 2008; Revised 2 February 2009; Accepted 4 March 2009

1. Introduction

It has been agreed that the Asian monsoon is dominated by three components, namely the South Asian monsoon, western North Pacific (WNP) monsoon and East Asian monsoon (Zhu and He, 1985; Zhu *et al*., 1986; Tao and Chen, 1987; Chen *et al*., 1991; Wang *et al*. 2001). As an important subcomponent of the Northern Hemisphere summer monsoon, the western North Pacific summer monsoon (WNPSM) bears a distinct signal of seasonal reversals of winds and large annual range of Outgoing Longwave Radiation (OLR; Murakami *et al*., 1992; Murakami and Matsumoto, 1994; Wang, 1994). Owing to the release of large amount of latent heat, the WNP becomes a major heating centre in the upper troposphere in summer (Yanai and Tomita, 1998) and therefore the convective activities there have considerable impact on the weather and climate over East Asia (Nitta, 1987). Moreover, the WNP wind anomalies and the associated equatorial zonal wind anomalies were shown to play active roles in the thermoline adjustment related to ENSO cycles, which has a direct feedback on the turnabout of ENSO (Wang *et al*., 1999).

The East Asian monsoon consists of South China Sea–western Pacific tropical monsoon and the Chinese mainland–Japan subtropical monsoon, with the boundary between them situated near 25°N (Zhu and He, 1985; Zhu *et al*., 1986; Chen *et al*., 2006). Correspondingly, the rotation styles of monsoon wind vectors in the two subsystems differ greatly from each other (Zhang and Li, 2007). Chen and Huang (2006) analyzed the vertical shears of climatological summer zonal wind in the East Asian monsoon domain and pointed out that there are positive vertical shears south of 25°N whereas they are negative north of 25°N. In addition, He *et al*. (2007) figured out that the onset of subtropical East Asian summer monsoon is earlier than that of the tropical WNP summer monsoon. They are independent of each other and the subtropical monsoon is not the northward branch of the tropical monsoon. Meanwhile, the South China Sea (SCS) summer monsoon is mainly affected by the

* Correspondence to: Jianping Li, LASG, Institute of Atmospheric Physics, Chinese Academy of Sciences, P.O. Box 9804, Beijing 100029, China. E-mail: ljp@lasg.iap.ac.cn

kinetic energy and convection coming from the tropical WNP (Chen *et al*., 2004). Therefore, the WNPSM plays an important role in the Asian monsoon system, which is different from that of subtropical East Asian monsoon.

The monsoon onset can be determined by the seasonal change in either surface winds or local rainfall (Tao and Chen, 1987; Ninomiya and Murakami, 1987; Lau and Yang, 1997; Webster *et al*., 1998; Krishnamurthy and Shukla 2000; Wang and Lin Ho, 2002, Zhang *et al*., 2002) because the monsoon climate is characterized by seasonal reversals of the winds and by a contrast between an intense rainy summer and a dry winter (Holland, 1986; Hsu *et al*., 1999; Lu and Chang, 1999; Li and Wu, 2000; Zhang *et al*., 2001; Wang *et al*., 2004). The WNPSM belongs to tropical monsoon, and its low-level winds reverse from winter easterlies to summer westerlies (Wang and Lin Ho, 2002). However, the local surface winds reversal and the dry to wet transition are not necessarily simultaneous (Wu and Wang, 2000; Wang *et al*., 2004); they are almost the same in the SCS monsoon onset, whereas they are different in the Indo-China peninsula (Matsumoto, 1997). Some research pointed out that the wind anomalies and pressure over the Philippine Sea and the SCS summer monsoon play a key role in linking ENSO and the East Asian climate (Wang *et al*., 2000; Chan and Zhou, 2005; Zhou and Chan, 2007). Therefore, the variations of abrupt wind change over the WNP could be a crucial factor affecting WNPSM, which deserves further study.

In addition, previously, attention has been mainly paid to the special migrations of climatological monsoon rainfall in the WNP. Some studies have shown the rainfall onsets over the WNP display distinct northeastward march (Murakami and Matsumoto, 1994; Wang, 1994). Matsumoto (1992) pointed out the multiple onset stages over WNP regions. The multiple onsets of summer monsoon in WNP have been investigated by a series of research (Ueda *et al*., 1995; Ueda and Yasunari, 1996; Wu and Wang, 2000, 2001; Ueda, 2005). And these multiple onsets are related to the different regions and they denote the special propagation of monsoon onsets. However, little attention has been paid to the local monsoon onsets, which are important for understanding seasonal variability for the WNPSM.

Atmospheric Model Intercomparison Project (AMIP) has provided a comprehensive evaluation of the performance of atmospheric general circulation models (AGCMs) and proved to be a useful benchmark of model sensitivity and predictability experiments to sea surface temperature (SST) forcing (Slingo *et al*., 1996; Boyle, 1998; Gates *et al*., 1999). However, current climate models have notable deficiencies in simulating the South Asian summer monsoon (Sperber and Palmer, 1996; Sperber *et al*., 2000). Although a wealth of effort has been directed towards developing and improving AGCMs, this effort has not been driven to a great extent by obtaining a proper simulation of the monsoon or its associated variability over the WNP. The performance of climate models in simulating the WNPSM is even poorer than that of the Indian Summer Monsoon (ISM) (Kang *et al*., 2002a,b). Soman and Slingo (1997) and Gadgil and Sajani (1998) have shown that the realistic simulation of variability in the WNP may be a key factor to simulate strong or weak monsoons that are associated with ENSO. Unfortunately, there are few studies on assessing the models' performance in simulating the seasonal variability of the WNPSM. In the present study, we examine the performance of current AGCMs in simulating the complex climatological variations of WNPSM, particularly the features of wind direction over the WNP, and try to find the common errors to improve the AGCMs.

This paper is organized as follows. Section 2 describes the observed data and model data as well as the definition of two-step wind onsets of monsoon. Section 3 examines the features of twice wind onsets and the corresponding circulation patterns. The relationships between twice wind onsets, OLR and rainfall are investigated in Section 4. Section 5 presents the simulations of AMIP models and Section 6 concludes this study with a brief summary of the results.

2. Data and methodology

The observed data used in the analysis and evaluation are the daily 850 hPa wind and geopotential height derived from National Center for Environmental Prediction-National Center for Atmospheric Research (NCEP/NCAR) reanalysis (Kalnay *et al*., 1996); the Merged Analysis of pentad (5-day mean) Precipitation from the Climate Prediction Center (CPC) (CMAP; Xie and Arkin, 1997) as well as the daily OLR of National Oceanic and Atmospheric Administration (NOAA) provided by Climate Diagnostics Center (CDC; Liebmann and Smith, 1996). The climatological data of these dataset are all constructed for the 21-year mean for 1979–1999 with global coverage on $2.5^\circ \times 2.5^\circ$ grids. Thirty-one days running mean of wind data and 5-points gauss filter of rainfall have been done in order to filter the short-time synoptic systems less than 30 days.

Recently, in preparation for the Intergovernmental Panel on Climate Change (IPCC) Fourth Assessment Report (AR4), more than a dozen international climate modelling centres conducted a comprehensive set of long-term simulations for AMIP, the climate in twentieth century and different climate change scenarios in the twenty-first century. AMIP is a standard experimental protocol for global AGCMs (see http://www-pcmdi.llnl.gov/projects/amip/index.php). It provides a community-based infrastructure in support of climate model diagnosis, validation, intercomparison, documentation and data access. The model output from AMIP simulation used for the IPCC AR4 have been acquired from different modelling groups and stored at the Program for Climate Model Diagnosis and Intercomparison (PCMDI). This analysis is based on AMIP simulations from seven AGCMs and Table I summarizes some descriptions of these models (see http://www-pcmdi.llnl.gov/ipcc/about_ipcc.php for more information

Table I. The information about AGCMs of AMIP in IPCC fourth assessment.

Model	Institution	Resolution	Simulated periods	Experiments
CNRM-CM3	Centre National de Recherches Meteorologiques, France	T42L45	1979–2000	1
GISS-MODEL_E_R	NASA Goddard Institute for Space Studies, America	4° × 5°L20	1979–2000	1
IAP-FGOALS-1.0g	LASG, Institute of Atmospheric Physics, China	2.8125° × 2.8°L26	1979–1999	3
INM-CM3.0	Institute for Numerical Mathematics, Russia	4° × 5°L21	1979–2003	1
MIROC3.2 (medres)	CCSR/NIES/FRCGC, Japan	T42L20	1979–2002	1
MPI-ECHAM5	Max Planck Institute for Meteorology, Germany	T63L32	1978–1999	3
MRI-CGCM2.3.2a	Meteorological Research Institute, Japan	T42L30	1979–2002	1

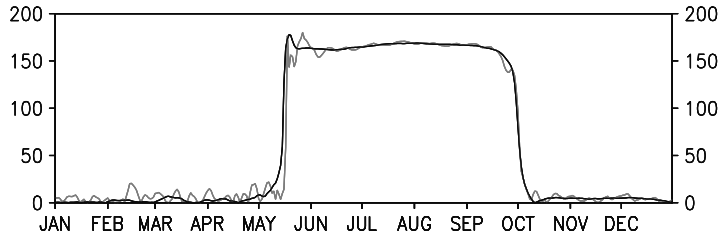

Figure 1. Seasonal variation of absolute angle of wind vectors at 15 °N, 60 °E. The grey line and black line denote the 5 days and 31 days running mean, respectively. Unit: degree.

about the models). Because of the various simulation periods in every model, model simulations of daily 850 hPa wind components and surface precipitation from 1 January 1979 to 31 December 1999 are averaged to construct the climatological annual cycle. Here IAP-FGOALS-1.0g and MPI-ECHAM5 are the ensemble mean of each single experiment.

Zhang and Li (2007) introduced a concept, the directed angle, to describe the seasonal variation of wind vector. It indicates that most of the wind vectors over WNP are clockwise to counter-clockwise rotations. As both the directed angle and absolute angle are good to reflect the seasonal reversal of monsoon, here we use the absolute angle (Li and Zeng, 2000; Zhang and Li, 2007) to analyze the wind direction of monsoon. January climatological wind vector is chosen as the reference wind vector.

The absolute angle between prevailing surface wind vectors is calculated as follows:

$$\beta_j = \beta(\mathbf{V}_j, \mathbf{V}_R) = \arccos\left(\frac{(\mathbf{V}_j, \mathbf{V}_R)}{|\mathbf{V}_j||\mathbf{V}_R|}\right), \quad (j = 1, \ldots, 365). \tag{1}$$

where $\mathbf{V}_j$ is the daily wind vector, and $\mathbf{V}_R$ is the reference wind vector at the same point. In this study we select January climatological wind vector (one, however, could choose other months) as the reference wind vector. The norm ($\mathbf{V}_j$, $\mathbf{V}_R$) means vector product, and $|\bullet|$ denotes the module of wind vector. Thus β_j essentially measures the contrast of the angles of wind vector between a specific daily and the corresponding winter. Obviously, $0 \leq \beta_j \leq 180^\circ$, that is, β_j is always positive, so it is named absolute angle.

Figure 1 shows an example of the curve of absolute angle for the point at (15°N,60 °E), and most tropical monsoon regions have the similar features. The curve increases slowly from January and the amplitudes are less than 15°, but they rapidly and obviously increase from early May. Towards mid-May, the increase suspends where a notable turning is shown and the curve enters a stable summer state. It denotes the first wind onset of monsoon. Then near late September, the curve abruptly decreases rapidly such that other obvious turning occurs and ends the summer states. It denotes the wind withdrawal of monsoon. And Figure 2(a) shows the scattered representation of normalized wind vector. It is obvious that the dots are dense in winter and summer, which suggest the wind vector has two stable states in northeasterly and southwesterly, respectively. And the wind vector oscillates with a small angle in its own state, but reverses rapidly from winter state to summer state. The process of wind vector rotation from winter to summer can be summarized in the schematic representation of Figure 2(b). It is apparent that the sudden change of wind direction is an important feature of monsoon onset. And the absolute angle is able to describe the variation of wind direction, and the turning corners on it are good to represent the abrupt transition of wind onset and withdrawal of monsoon.

3. Twice wind onsets of monsoon and related variations of OLR and rainfall

3.1. The phenomenon of twice wind onsets for monsoon

The fundamental characteristics of monsoon are the annual winds reversal and dry and wet alternations. The summer monsoon onset is characterized by a sudden wind reversal and a dry to wet transition. Based on the definition of wind onset, the abrupt variations of

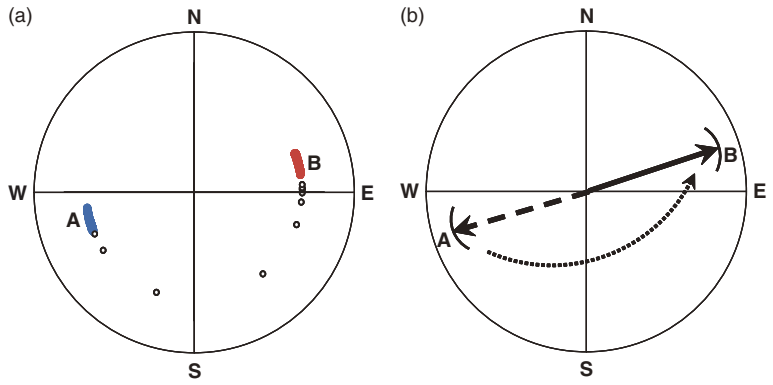

Figure 2. Phase representation of wind direction from winter to summer at 15 °N, 60 °E. (a) Scattered representation of normalized wind vector: blue solid dots represent winter state (Day 1 ~ 132), hollow dots represent transitional season (Day 133 ~ 143), red solid dots represent summer state (Day 144 ~ 255). (b) Schematic representation. Radium A and B denote small oscillation in winter and summer states respectively. This figure is available in colour online at www.interscience.wiley.com/ijoc

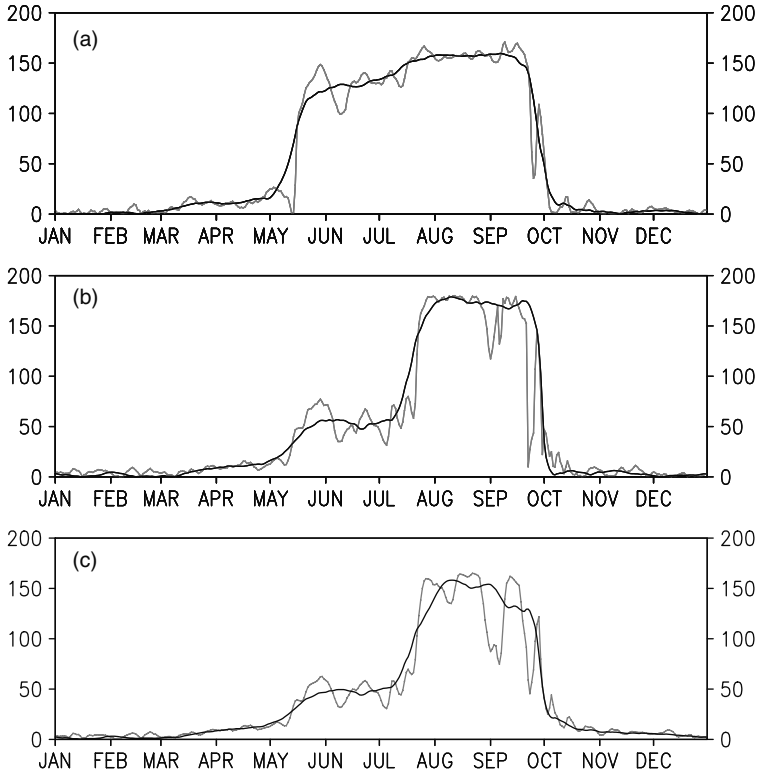

Figure 3. The same as in Figure 1 except for the following locations: (a)15 °N, 120 °E; (b) 15 °N, 130 °E; (c) 15 °N, partial zonal average between 125° and 140 °E.

wind directions are well described in the Asian monsoon regions. Meanwhile, a larruping feature of wind direction evolution is found for WNPSM over the WNP of 10°–22.5 °N, 125°–145 °E.

Figure 3(a) indicates the absolute angle evolution at (15°N, 120 °E) in the SCS, which is similar to the point at (15°N, 60 °E). The wind vector has two stable states (winter state and summer state) and the switch between these two states is very swift. However, at (15°N, 130 °E) [Figure 3(b)] the variation of wind direction is much different from the point at (15°N, 120 °E). The curve of absolute angle increases slowly from January with small amplitudes near 10°, then increases suddenly and rapidly from May. Towards mid-May, the increase suspends when a notable turning is shown and then the curve enters a stable state (defined as mid-state). After keeping the stable state for more than 50 days, the curve increases quickly again in mid-July and soon enters another stable state (summer state). This state is maintained for about 2 months before decreasing and ending the summer state in late September. Figure 4(a) shows scattered wind direction of normalized wind vector; it is notable that the dots centralize in three belts. There are other dense belts in addition to winter and summer states, named mid-state here. It suggests that the wind vector shows northeasterly and oscillates with a small angle for a

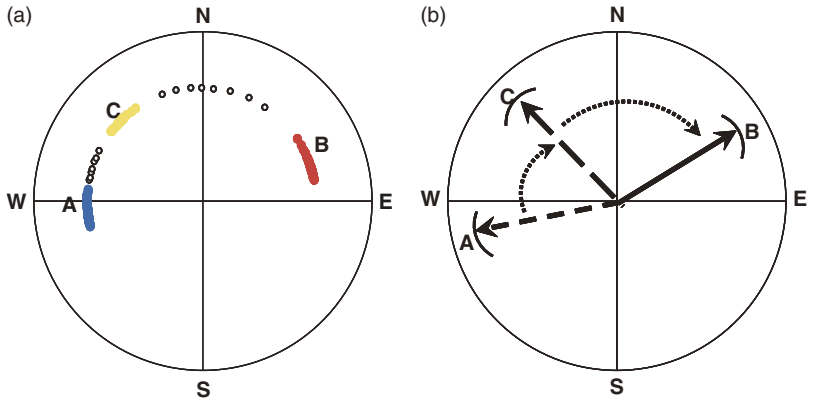

Figure 4. The same as in Figure 2 except for the location at 15 °N, 130 °E. (a) Blue solid dots represent winter state (Day 1 ~ 125), yellow solid dots represent mid-state (Day 133 ~ 191), hollow dots represent transitional seasons (Day 126 ~ 132 and Day 192 ~ 199) and red solid dots represent summer state (Day 200 ~ 271). (b) Radium C denotes small oscillation in mid-state. This figure is available in colour online at www.interscience.wiley.com/ijoc

period in A (winter state), then rotates to C (mid-state) rapidly, which implies the occurrence of the first wind onset. After oscillating for a period with southeasterly in position C (mid-state), the wind vector switches to B (summer state) rapidly and turns to southwesterly, which implies the occurrence of the second wind onset. For better understanding the evolutionary process of wind vector a schematic representation is shown in Figure 4(b). That phenomenon shows that twice wind onsets during the evolution of wind direction from winter to summer are quite different from that in other Asian monsoon regions. The zonal mean absolute angle between 125° and 140 °E at 15°N is shown in Figure 3(c). It also has similar feature of the twice wind onsets as in Figure 3(b), and indicates a stable state with the angle near 50° before mid-July. As this feature of wind onset has not been found in surrounding areas, it suggests that the twice wind onsets is a typical feature for the variations of wind directions in these areas.

For better investigating the differences of special variations of wind direction between the WNP and its surrounding area, Figure 5 shows the time–latitude cross sections of annual absolute angle at 120 °E, 130 °E and the zonal mean between 125° and 140 °E. It obviously indicates that the dense isoline belts appear near mid-May and late October at 15°N, which represent the wind onset and wind withdrawal of monsoon, respectively [Figure 5(a)]. That also suggests the wind onset of monsoon just occurs once before withdrawal. For Figure 5(b), there are three dense isoline belts, and two of them appear before monsoon withdrawal, which also confirm the occurrence of twice wind onsets as shown in Figure3(b) and (c). The first dense isoline belt is near early May at 17.5 °N and near late May at 10°N, which indicates a little southward propagation. Moreover, the onset starts earlier at higher latitude than low latitude for the first wind onset. However, the second dense isoline belt is quite different from the first one and its position is near late June at 10°N but near late July at 17.5 °N, which has a notable northward propagation. During the twice wind onsets, the absolute angles of wind vectors are stable around 40°–65°. In addition, the periods of maintaining this stable state have regional distinctions. And the time interval indicates short to long from south to north, which looks like an inverse trapezium. The time–latitude cross section of zonal mean between 125° and 140 °E has the same pattern as that of 130 °E [Figure 5(c)]. There are also two dense isoline belts except the one that represents wind withdrawal of monsoon and the positions of these two belts are consistent with those of 130 °E, which suggests that the variations of wind directions in these regions have similar features.

3.2. The relationships between twice wind onsets of monsoon and the variations of rainfall and OLR

Over the WNP, there is a large annual range of OLR (Murakami and Matsumoto, 1994) and heavy rainfall abruption (Wang and Lin Ho, 2002; Wu and Wang, 2001). The climatological pentad mean OLR shows a clear transition from the dry to the wet regime and the wet regime is sustained after the onset. The monsoon rainy onset is an abrupt phenomenon and the climatological rainy onset displays three distinct stages (Wu and Wang, 2001). This section focuses on the annual variation of OLR and surface precipitation compared to the corresponding twice wind onsets.

Figure 6(a) displays climatology of the OLR seasonal variation at (15°N, 130 °E) and (20°N, 130 °E). For the 15°N, the wet regime starts from mid-June when the OLR sustains below 240 W/m^{-2} and shows one wet state. But at (20°N, 130 °E), the OLR variation is much different from the former. There are notable double peaks near late May and late July, which imply the two transitions from the dry to the wet regime. Moreover, the dates of transition are consistent with those of the twice wind onsets at (15°N, 130 °E). And the zonal averages between 125° and 140 °E at 15°N and 20°N are similar [Figure 6(b)]. There are double peaks at the 20°N and just one peak at 15°N. Figure 7 indicates the evolution of surface precipitation. It is obvious that the double peaks of rainfall coincide with the OLR not only at (20°N, 130 °E) [Figure 7(a)] but also for the zonal

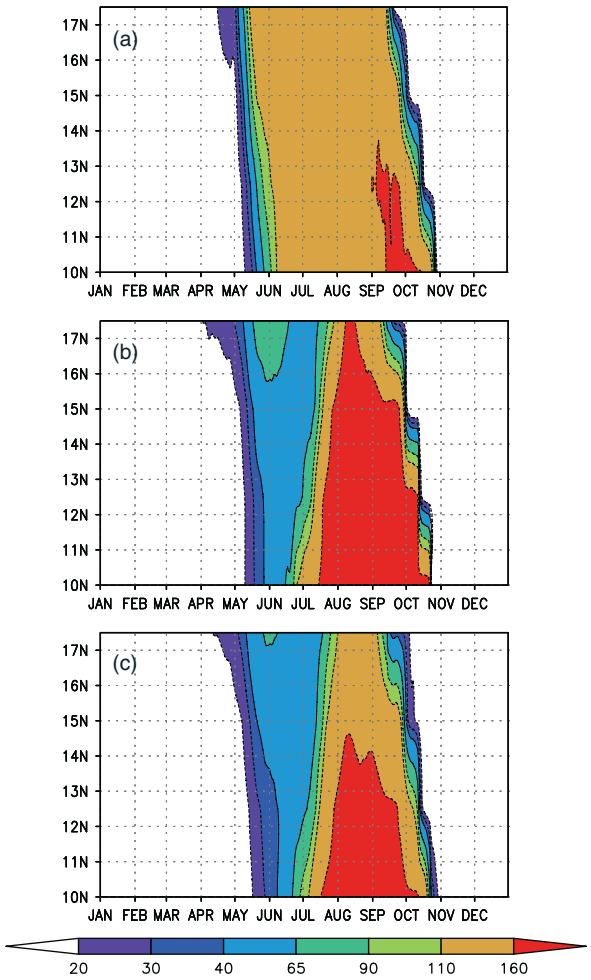

Figure 5. The time–latitude cross sections of absolute angle (degree) at (a)120 °E; (b)130 °E; (c) the partial zonal average between 125° and 140 °E. This figure is available in colour online at www.interscience.wiley.com/ijoc

average between 125° and 140 °E at 20°N [Figure 7(b)]. The first peak is shown in late May and the second peak starts from late July. Similarly, the rainfall variations do not show double peaks at 15°N. It may suggest that the areas where the variations of OLR and rainfall respond to the twice wind onsets are shifted to the north about 5° latitude. Figure 8 shows the rainfall temporal distribution to corresponding wind direction with 5° latitude discrepancy. It is easy to find that the heavy rainfall is located in two belts related to corresponding dense dots in B (summer state) and C (mid-state). So the first wind onset also induces a peak value of rainfall. Therefore, the first wind onset of monsoon over WNP may be important to influence the precipitation in the northern neighbouring regions.

In order to investigate whether there are corresponding patterns as Figure 5 in the whole of WNP, the time–latitude cross sections of OLR and rainfall from 15°N to 22.5 °N are shown in Figure 9. It displays that to the north of 5°, the OLR and rainfall have the same pattern that is similar to that of the absolute angle. When the first wind onset occurs, the OLR is 235–255 W/m^{-2} [Figure 9(a) and (b)] and rainfall is maintained at 3–6 mm/day [Figure 9(c) and (d)] for a period in most regions. After the second wind onset of monsoon, the OLR soon decreases below 235 W/m^{-2} and maintains lower values in the long term. Meanwhile, the precipitation becomes intense and enters the heavy rainfall season. It is simultaneous for the first onsets of OLR and rainfall from 15°N to 22°N, but the first wind onset propagates from north to south. Therefore, the propagating direction of the first wind onset is different from that of OLR and rainfall. Comparatively, the second wind onset is a little earlier than that of the other two. Moreover, the OLR and rainfall propagate from south to north as that of the second wind onset. Thus, they all look like the inverse trapeziums. In addition, a bigger value belt appears in the north between the first and the second wind onsets (Figure 5). Also, similar phenomena display in OLR and rainfall, which confirms that the twice wind onsets may lead to a similar pattern for the

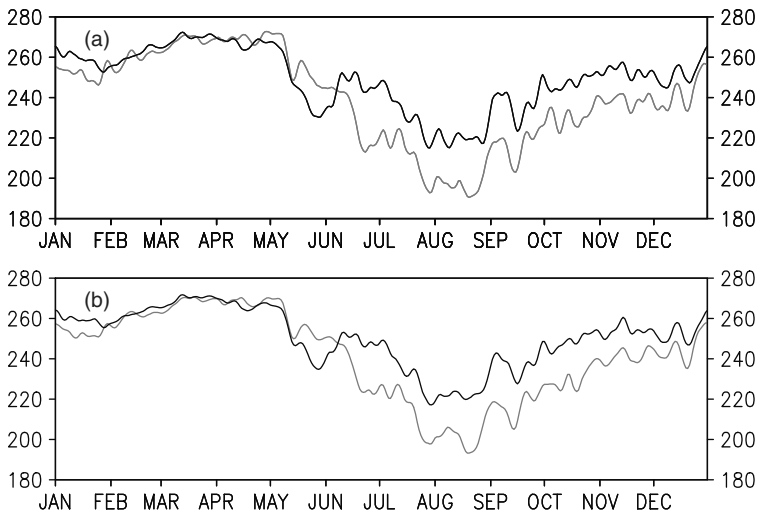

Figure 6. Seasonal variation of OLR (W/m^2) at (a) 130 °E; (b) partial zonal average between 125° and 140 °E. The black thick line and grey thin line denote OLR at 20 °N and 15 °N, respectively.

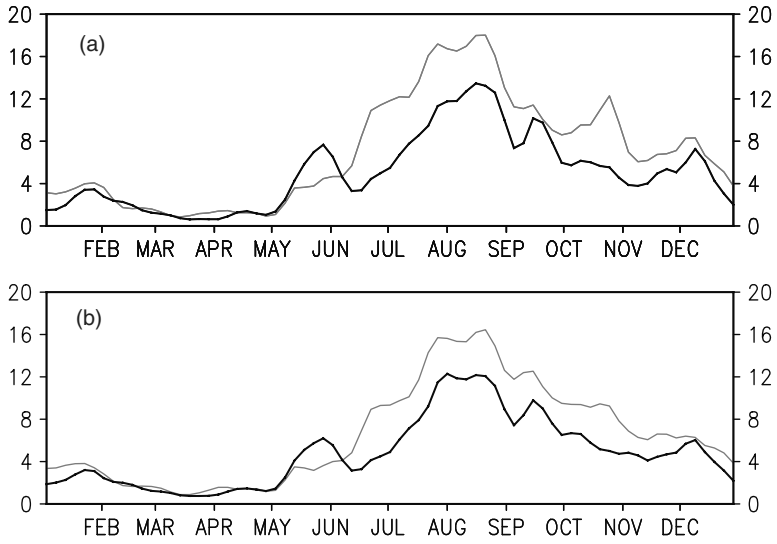

Figure 7. The same as in Figure 6 except for the surface precipitation (mm/day).

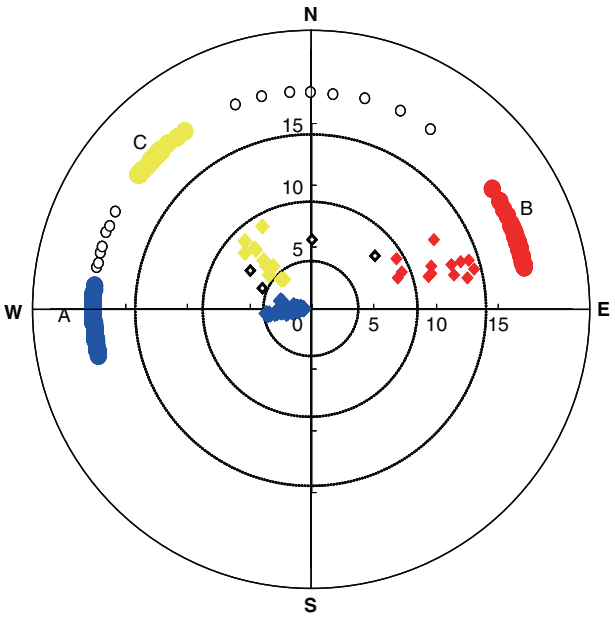

Figure 8. The same as in Figure 4 except for the scattered representation of surface precipitation at 20 °N, 130 °E to corresponding wind direction at 15 °N, 130 °E. The green solid dots denote precipitation (mm/day). This figure is available in colour online at www.interscience.wiley.com/ijoc

OLR and rainfall in the northern adjoining region about 5° latitude again. It suggests that the influence of wind direction of monsoon is not a local effect. Therefore, over the WNP, the climatological variations of wind direction undergo two abrupt changes in summer, which are the characteristic features of monsoon onsets, and have significant impact on the northern neighbouring convection and rainfall.

4. The circulation feature during the twice wind onsets

As the twice wind onsets is a particular feature for the WNP, it is important to separate the corresponding phase to examine the circulation. From the curve of annual absolute angle of the representative point at (15°N, 130 °E), four phases can be easily divided based on the dates of the twice wind onsets and wind withdrawal as follows: (1) Phase 1 (pentad 1 to 24); (2) Phase 2 (pentad 29 to 37); (3) Phase 3 (pentad 43 to 52); (4) Phase 4 (pentad 55 to 73). Phase 1 and Phase 4 should be the identical states based on the wind direction. However, the OLR and rainfall characteristics are quite different in the periods before monsoon onset (Phase 1) and after monsoon withdrawal (Phase 4; Figures 6 and 7). Therefore, the annual cycle has been divided into four phases based on the dates of the twice wind onsets and wind withdrawal and Phase 1 and Phase 4 belong to winter states, Phase 2 is the summer state I, and Phase 3 is the summer state II.

The lower-lever (850 hPa) circulation and surface precipitation during the four phases are first considered. The composite 850 hPa geopotential height and rainfall in the four phases are shown in Figure 10. The western Pacific subtropical high (WPSH) covers the spacious ocean to the east of Indo-China including the Philippine Sea in Phase 1 [Figure 10(a)]. The ridge of the WPSH extends westward reaching Indo-China. A low is located in southwestern China. And the primary rainbelts are over the southeast of China and the Eastern Sea as well as the location of Inter-tropical Convergence Zone (ITCZ) in the vicinity of the equator. A high exhibits in the WNP at 200 hPa (figure not shown). Meanwhile, Figure 11(a) indicates the vertically integrated moisture flux and the divergence in Phase 1. The northeasterlies control much of the SCS and the Philippine Sea whereas southwestern China is covered by southwesterlies as well as intense moisture convergence. During Phase 2 [Figures 10(b) and 11(b)], the circulation patterns are quite different from Phase 1. And the wind onset date is close to the onset of SCS monsoon (He *et al*., 2007). The WPSH retreats northeastward and the ridge exhibits southwest–northeast direction. In China,

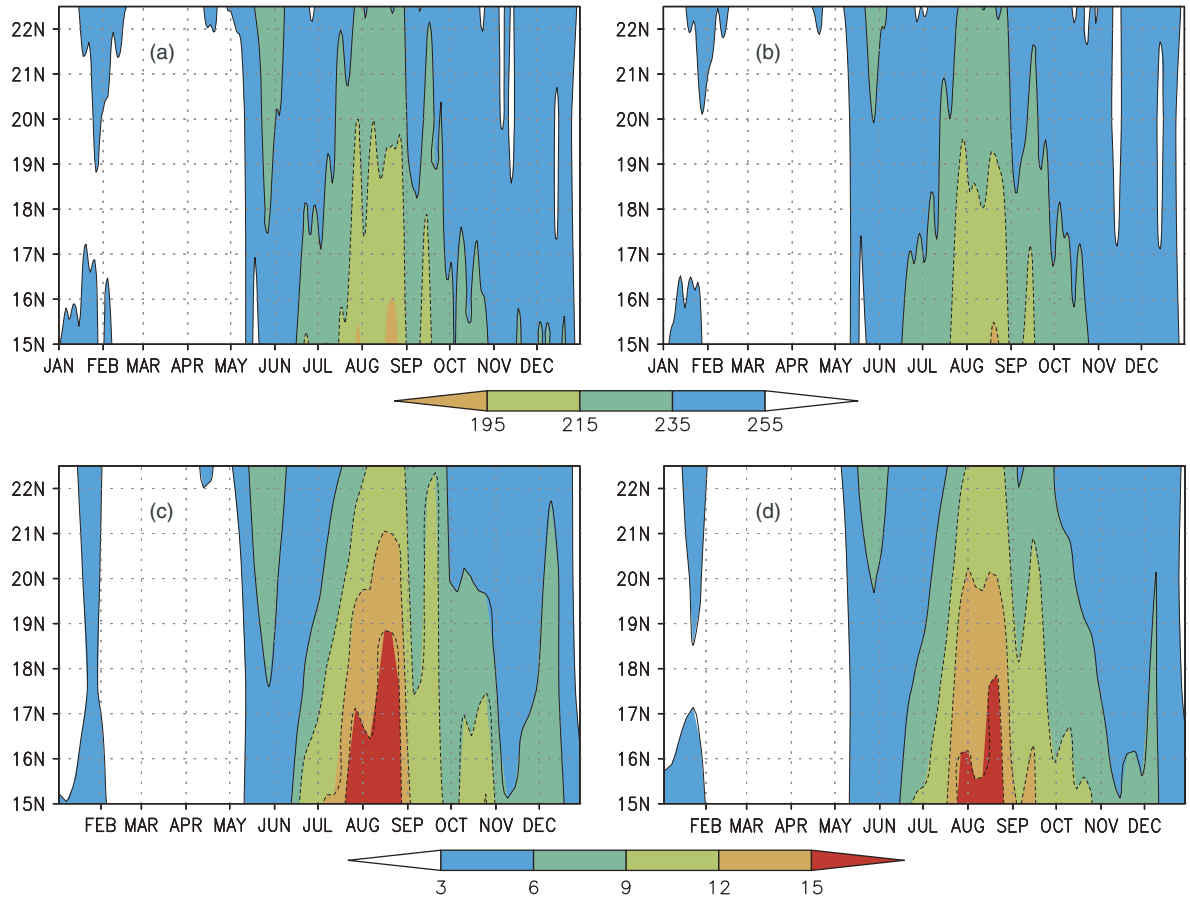

Figure 9. The time–latitude cross sections of OLR (W/m^2) at (a)130 °E; (b) partial zonal average between 125° and 140 °E, and surface precipitation at (c)130 °E; (d) partial zonal average between 125° and 140 °E. This figure is available in colour online at www.interscience.wiley.com/ijoc

the primary rainbelts cover South China influenced by a strong moisture flux of southwesterlies, which are consistent with the starting period of pre-flood rainy season over South China (Chen *et al*., 2000). Meanwhile, a strong moisture flux induced by the cross-equatorial flows affect the SCS without reaching the WNP as the ridge of WPSH is controlling there. Thus, a monsoon trough extending from southwest China accompanies heavy rainfall and intense moisture convergence present in the middle of the SCS, and the southwesterlies cover the whole of SCS. Comparatively, the Philippine Sea is in the southwestern edge of WPSH and controlled by southeasterlies. Meanwhile, a weak monsoon trough begins exhibiting in the WNP near the equator. The high over the WNP disappears and the South Asian high at 200 hPa exhibits and enhances (figure not shown). Also, the moisture convergence is not much intense and the heavy rainbelt is still located on the southeast to this area. At the same time, the cross-equator flows encounter the easterly flows over the WNP. The WPSH migrates northward and the ridge reaches about 30°N in Phase 3 [Figure 10(c)]. A notable transverse monsoon trough and strong moisture convergence present over the WNP where another maximum precipitation also appears at the same time [Figure 11(c)]. And this eastward march of the monsoon trough and the high convective instability zone are related to the seasonal migration of the warm SST centre in the SCS and the Philippines (Wu and Wang, 2001). On the other hand, the SCS is still controlled by a strong moisture flux and intense moisture convergence, which is accompanied by maximum precipitation, too [Figure 11(c)]. Moreover, the cross-equatorial flows are strong enough to influence large range of areas except the SCS. As a result, the WNP is covered by southwesterlies with high moisture convergence. In the subtropics, the heavy rainbelts migrate to Korea and Japan. The South Asian high at 200 hPa migrates northwestward (figure not shown). In Phase 4, the WNP monsoon trough disappears and the precipitation weakens in the spacious tropical regions such as the SCS and the WNP [Figure 10(d)]. The high in WNP at 200 hPa exhibits again (figure not shown). At the same time, the moisture convergences in these areas also decrease with the appearance of northeasterlies [Figure 11(d)]. The corresponding compositions of 500 hPa geopotential height are similar to that of 850 hPa (figure not shown).

As the special variation of the ridge of WPSH plays an important role in the twice wind onsets of monsoon from the above composite analysis, the time–longitude cross section of 850 hPa geopotential height and latitude along the ridge of WPSH is shown in Figure 12 to examine the migration of WPSH. In early May before the first wind

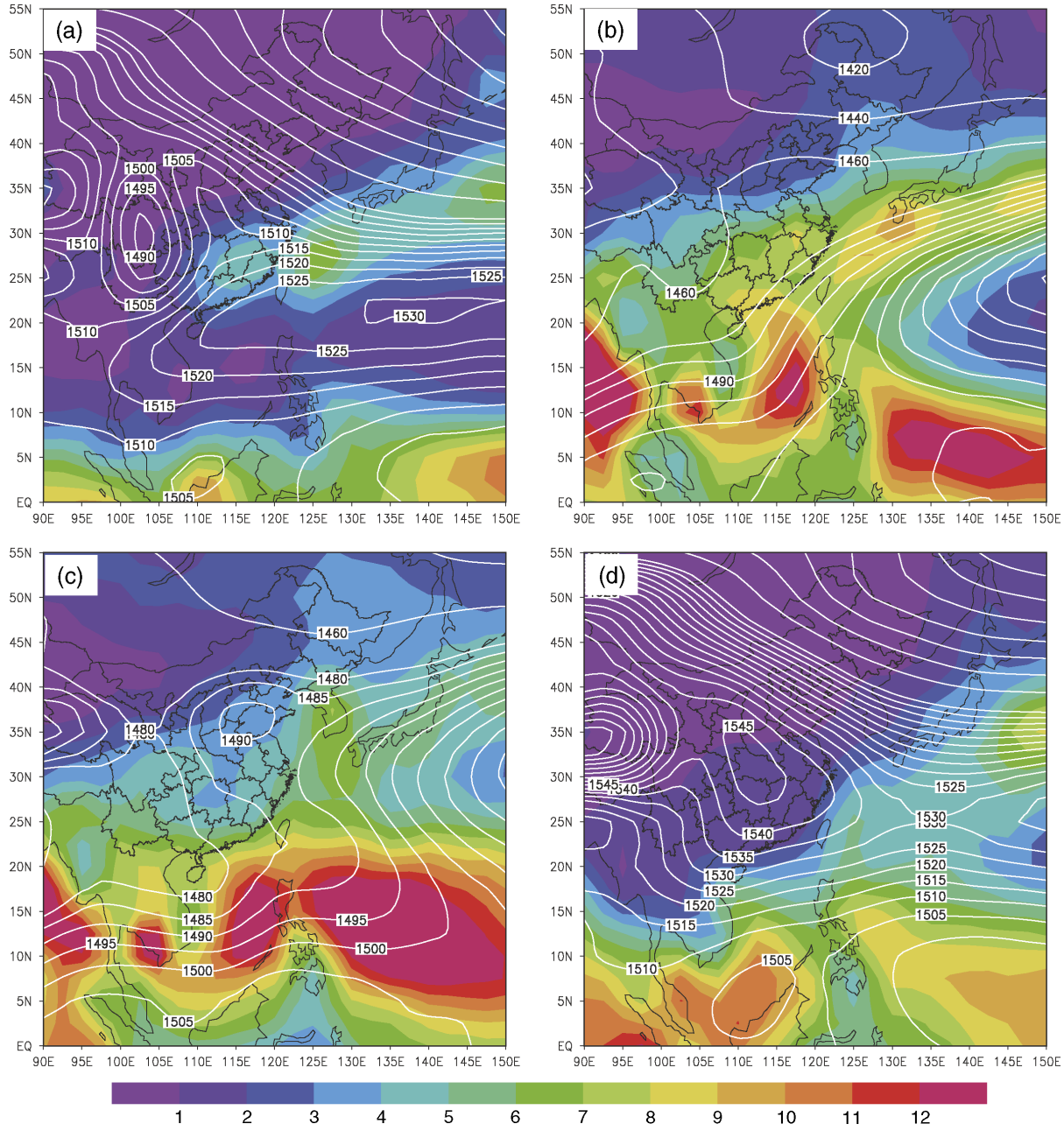

Figure 10. The composite 850 hPa geopotential height (m, contour) and surface precipitation (mm/day, shaded) in (a) Phase 1 (pentad 1 to 24); (b) Phase 2 (pentad 29 to 37); (c) Phase 3 (pentad 43 to 52); (d) Phase 4 (pentad 55 to 73). This figure is available in colour online at www.interscience.wiley.com/ijoc

onset, a notable eastward retreat occurs [Figure 12(a)]. Meanwhile, the ridge of WPSH turns from west–east to southwest–northeast direction and is stable for a period [Figure 12(b)]. That may be the possible reason for the wind direction being stable after the first wind onset [Figure 3(b) and (c)]. Then the WPSH retreats eastward again in early July, and the ridge suddenly jumps to 30°N in late July. That would be the trigger to induce the second wind onset. The variation of the monsoon trough along the zonal average between 125°E and 140°E is shown in Figure 13 to examine its spatial variations. It indicates that the trough migrates to the north from 30 June to 31 July, which matches the second wind onset well. Therefore, the migration of the monsoon trough in the WNP may be a key factor to influence the second wind onset and induce heavy rainfall.

5. The performance of AGCMs in simulation of the twice wind onsets in the tropical WNP

The present model intercomparison has been focused on South Asian monsoon simulation with less attention paid to the WNPSM, a region perhaps crucial for the global climate system. The results derived from the present analysis show that the twice wind onsets of monsoon in the WNP is a characteristic phenomenon consisting of integrated monsoon system. This section examines how

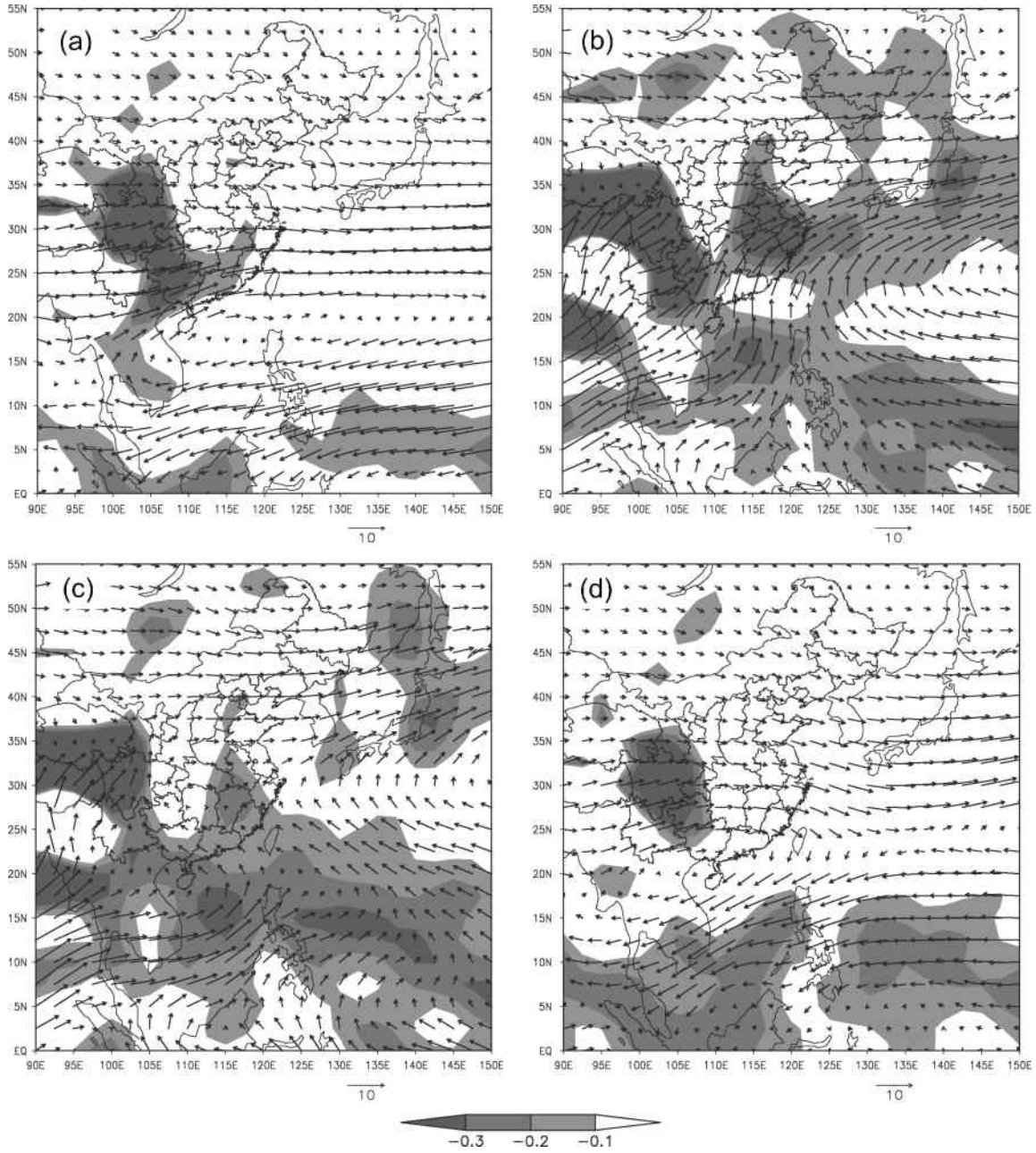

Figure 11. The same as in Figure 10 except for the vertically integrated moisture flux (kg/ms, vector) and its divergence (10^{-5}/s, shaded).

well the models simulate the climatological twice wind onsets and the corresponding rainfall pattern in the WNP.

To illustrate the general characteristics of twice wind onsets of monsoon simulated by the AGCMs under study, Figure 14 exhibits time–latitude cross sections of annual absolute angle for model simulations at 130 °E and the zonal average between 125 °E and 140 °E. It is clear that none of the models, including the ensemble mean, reproduces the twice wind onsets well either in 130 °E or the zonal average between 125° and 140 °E. Fortunately, MPI-ECHAM5 capturing part of a similar pattern through the timing is approximately 1 month ahead of its onset. Moreover, the simulated details differ from one model to another. Most of models, such as CNRM-CM3, IAP-FGOALS-1.0g, INM-CM3.0 and MIROC3.2 (medres), just have one dense isoline belt near June to July before monsoon withdrawal. Though GISS-MODEL_E_R is able to simulate two dense isoline belts that represent the twice wind onsets of monsoon, the patterns and the times when twice wind onsets occur are quite different from those observed. For MRI-CGCM2.3.2a, the simulation dates of the first is earlier than that of observation; moreover, the second wind onset and the stable state between onsets are not reproduced well. In addition, the grads of the isolines during the wind onset is much smaller compared to the observation. Comparatively, the simulation of MPI-ECHAM5 is close to that observed with two obviously dense isoline belts generally matching the wind onset of monsoon though the simulated second wind onset is a little earlier than observation. There

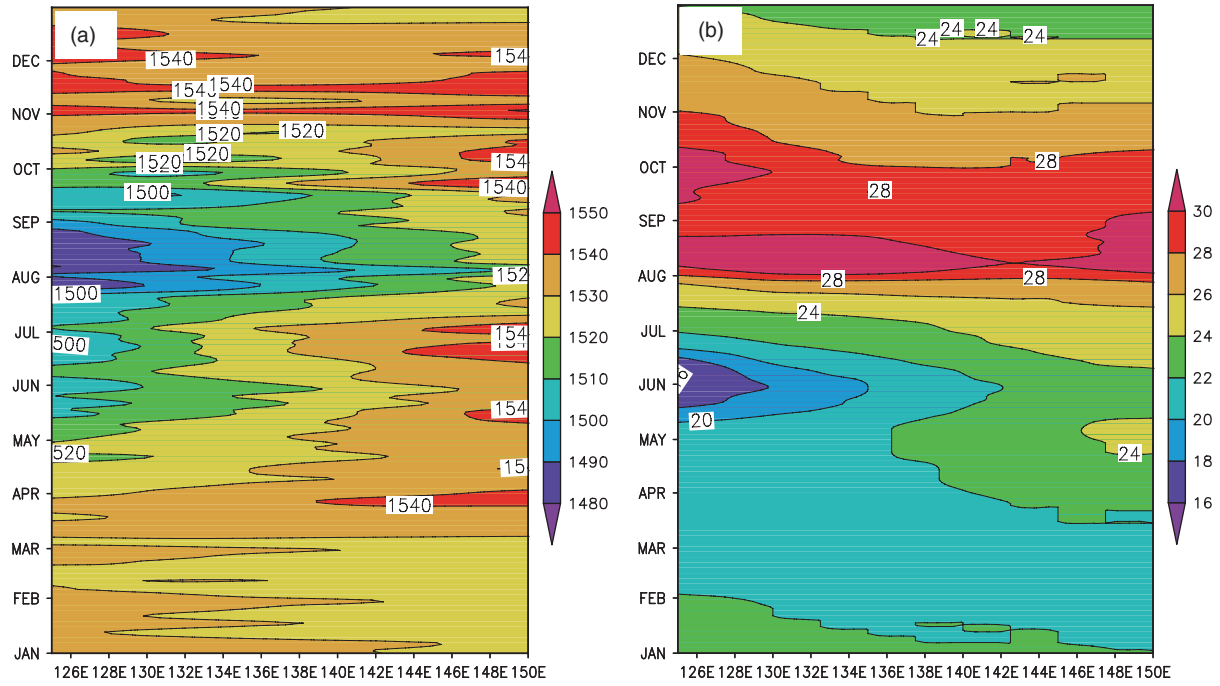

Figure 12. The time–longitude cross section of (a) geopotential height (m) and (b) latitude (°N) along the ridge of the western Pacific subtropical high at 850 hPa. This figure is available in colour online at www.interscience.wiley.com/ijoc

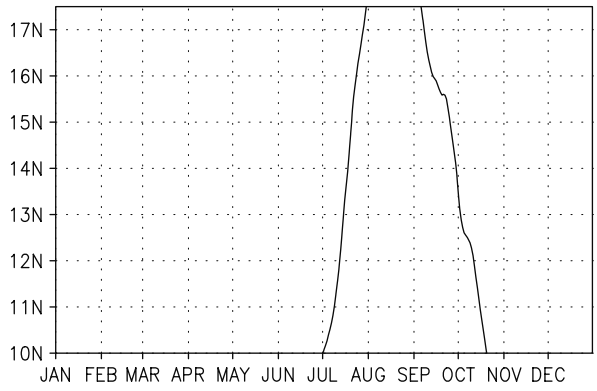

Figure 13. The time–latitude cross section of the 850 hPa monsoon trough over the WNP of partial zonal average between 125° and 140 °E.

are no improvements in the multi-model simulations of ensemble mean owing to the large discrepancies for all the models.

The ridge of the WPSH is good to describe the migrations of WPSH (Li and Chou 1998; Zhan *et al.*, 2008). From the simulated time–latitude cross section of the ridge of 850 hPa WPSH along the zonal average between 120° and 150 °E (figure not shown), all simulations except GISS-MODEL_E_R show that the ridge of WPSH migrates to 30° earlier than that observed. It may result in poor simulations in the second wind onset. Figure 15 displays the simulated migration of the WNP monsoon trough. None of the models is able to reproduce the evolution of the monsoon trough from south to north reasonably well. It may be related to the poor simulations of the date of the second wind onset for all models. And the simulated dates are earlier than those of the observations in the group model such as CNRM-CM [Figure 15(b)], GISS-MODEL_E_R [Figure 15(c)], MIROC3.2 (medres) [Figure 15(f)], MPI-ECHAM5 (Figure 15(g)] and MRI-CGCM2.3.2a [Figure 15(h)]. In addition, IAP-FGOALS-1.0g [Figure 15(d)], INM-CM3.0 (Figure 15(e)] and GISS-MODEL_E_R can not capture the trough completely in the area. Moreover, what the GISS-MODEL_E_R simulate is unrealistic because it does not extend to the north of 17.5 °N and it appears later than that observed in the migration from south to north. The simulated trough matches its simulated second wind onset well, which also confirms that the monsoon trough is very important for the second wind onset.

The time–latitude cross sections of the precipitation shifted to the north about 5° simulated by seven representative models of AMIP AR4 are shown in Figure 16. It shows that most models can not correctly depict the broad features of the variation of rainfall in the region. Moreover, regional details differ from one model to another. For example, the precipitation simulated by the CNRM-CM model has quite different characteristics from others that simulated excessive precipitation before monsoon onset. And the simulated heavy rainfall is maintained longer than that observed from July to September without extending northward enough, which may associate with the unreasonable simulation of absolute angle in the same period. GISS-MODEL_E_R and IAP-FGOALS-1.0g can not capture the intensity of precipitation in low latitude and simulate very weak rainfall. Besides, both of them produce an unrealistic heavy rainfall in winter. And the maximum rainfall simulated by INM-CM3.0 is not near 15°N but shifts to 20°N. MIROC3.2 (medres) also can not reproduce the precipitation intensity in summer. However, MRI-CGCM2.3.2a simulates excessive rainfall

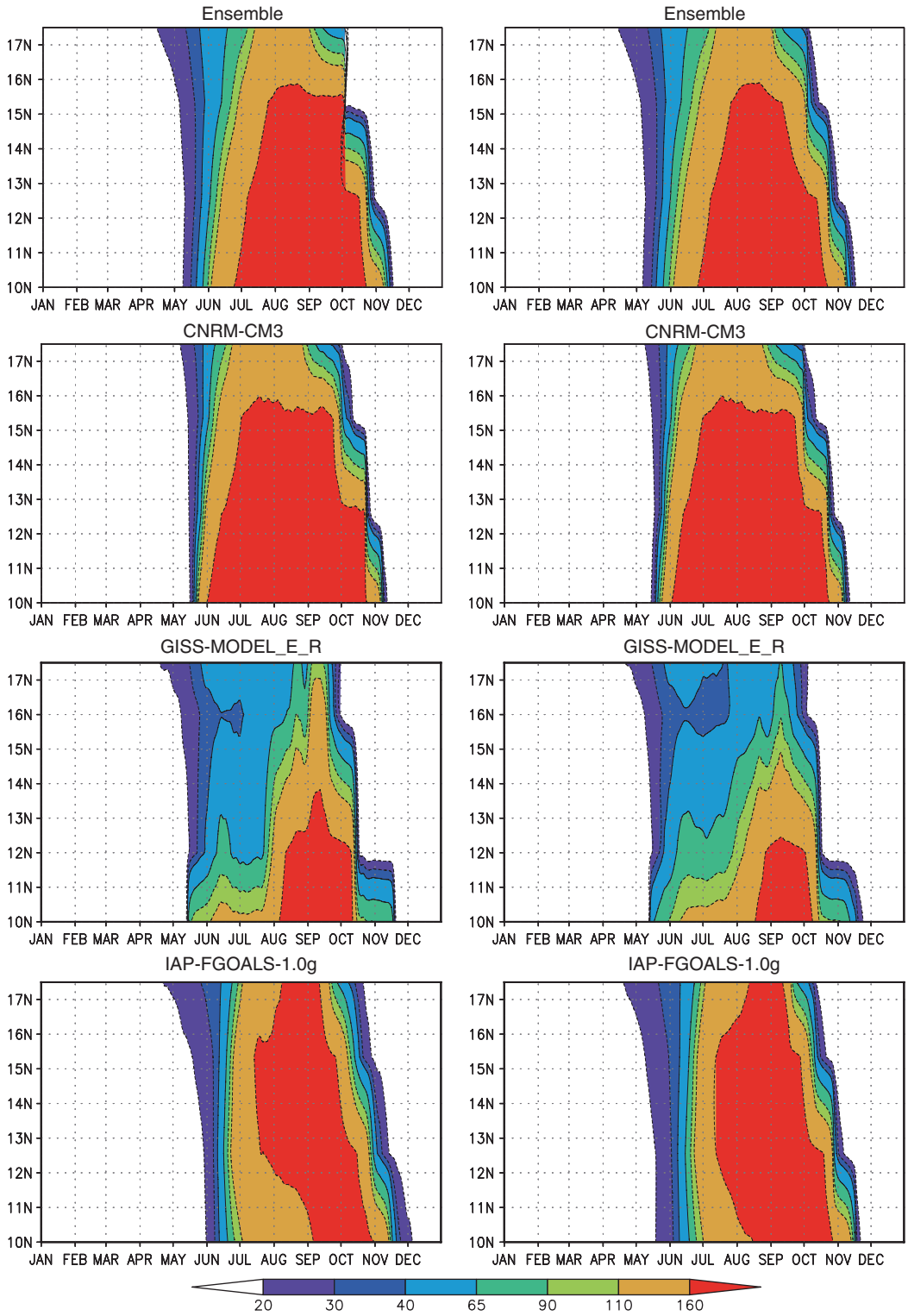

Figure 14a. The same as in Figure 5(b) and (c), but for the model simulations. The left line denotes the location at 130 °E and the right line denotes the partial zonal average between 125° and 140 °E. This figure is available in colour online at www.interscience.wiley.com/ijoc

that lasts from August to October and extends to 20°N. In addition, it indicates an unrealistic peak near June. Although the simulations of MPI-ECHAM5 are close to that observed in the precipitation intensity before monsoon withdrawal comparatively, many details are still needed. Therefore, there is no model having the ability to reproduce the rainfall variation corresponding to the twice wind onsets. Figure 17 shows the simulated rainfall in the area averaged in the domain of 15°–22.5 °N, 125°–140 °E; none of the models reproduces annual variations well. MRI-CGCM2.3.2a captures similar double peaks, but the dates and values are not consistent with that observed. Liang *et al*. (2001) have confirmed that wind biases are significantly correlated with those in

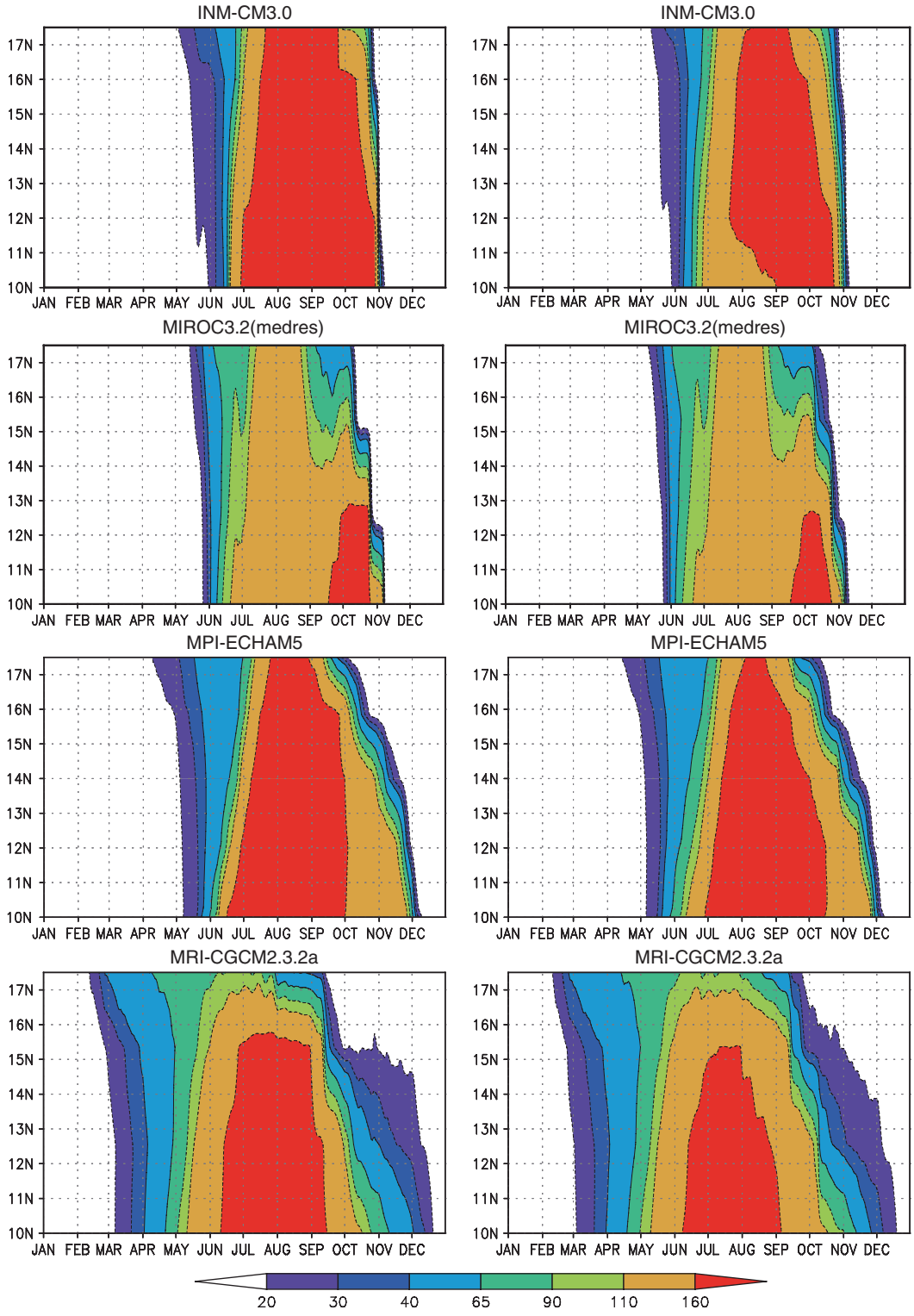

Figure 14. (*Continued*).

precipitation. And it is possible that the poor simulation of twice wind onsets of monsoon in WNP contribute to the poor results for precipitation simulation.

6. Summary and discussion

In this study, the larruping phenomenon on wind direction of WNPSM is revealed and examined. The results show that the WNPSM undergoes twice wind onsets before wind withdrawal. After the first wind onset occurring near mid-May at 15°N, the wind vector sustains in a stable state of southeasterly for a period of more than 50 days. In mid-July, the wind vector switches to southwesterly rapidly, which indicates the occurrence of the second wind onset, and then enters another stable state from late July. Over the entire west coast of Philippines, the rainfall

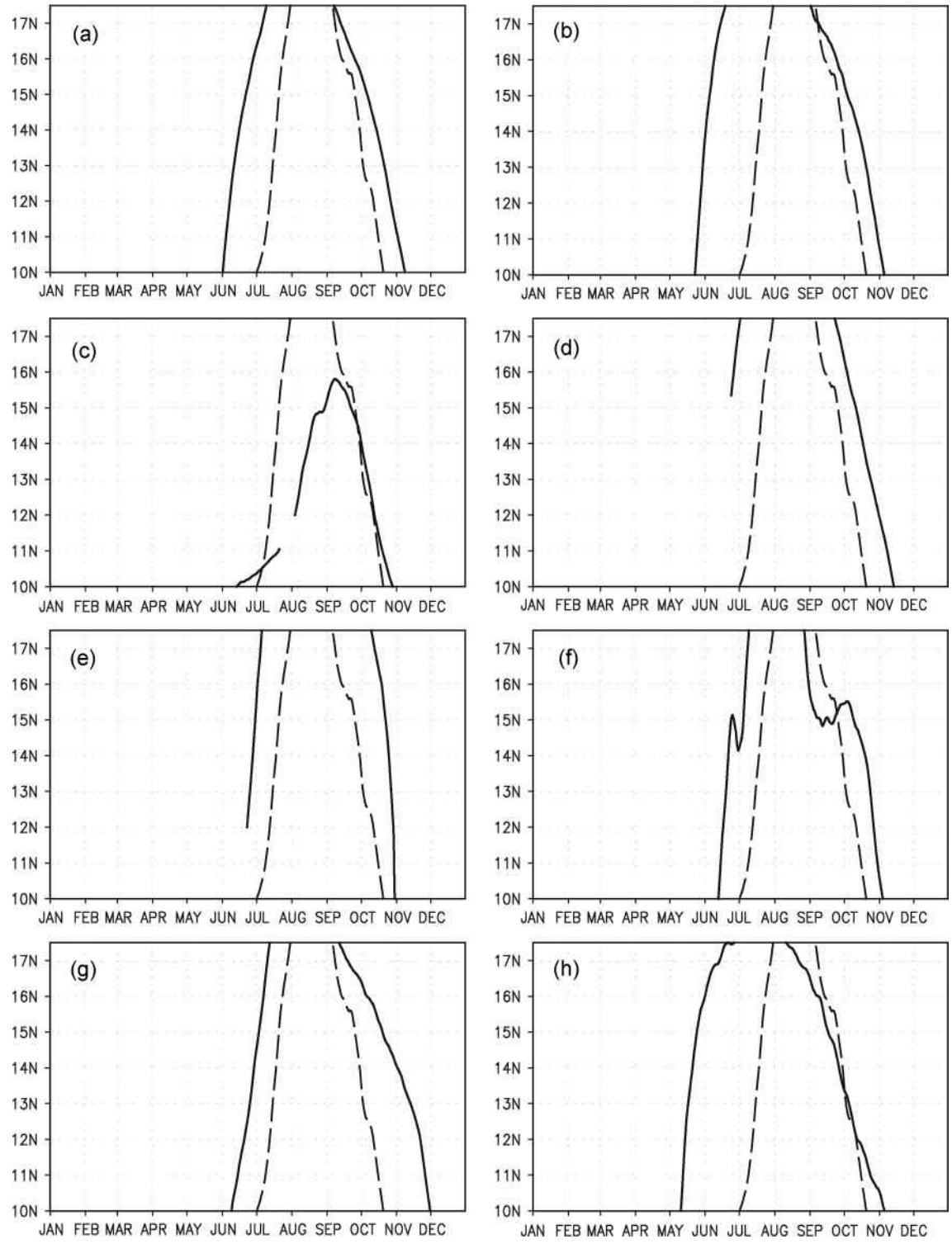

Figure 15. The same as Figure 13, but for the observation (dashed line) and model simulations (solid line). (a) Ensemble; (b) CNRM-CM3; (c) GISS-MODEL_E_R; (d) IAP-FGOALS-1.0g; (e) INM-CM3.0; (f) MIROC3.2 (medres); (g) MPI-ECHAM5; (h) MRI-CGCM2.3.2a.

increases steeply in mid-May and the maximum rainfall is shown from late July, which is consistent with the date of twice wind onset (Matsumoto, 1992; Akasaka *et al*., 2007). Moreover, Wu and Wang (2000, 2001) pointed out that around mid-May, monsoon rainfall commences in the SCS and the Philippines and the rainy season starts in the northeastern part of the WNP after mid-July. And the abrupt northward convection jump over WNP also appears near pentad 42 (late July) after the second wind onset (Matsumoto, 1992; Ueda *et al*., 1995; Ueda and Yasunari, 1996). In addition, the date of the twice wind onset coincides with the first transition of the Asian summer monsoon (mid-May) and the mature phase of ITCZ (mid-June) to the east of Philippines (Ueda, 2005).

The time–latitude cross sections of annual absolute angle at 130 °E and the average of 125°–140 °E indicate

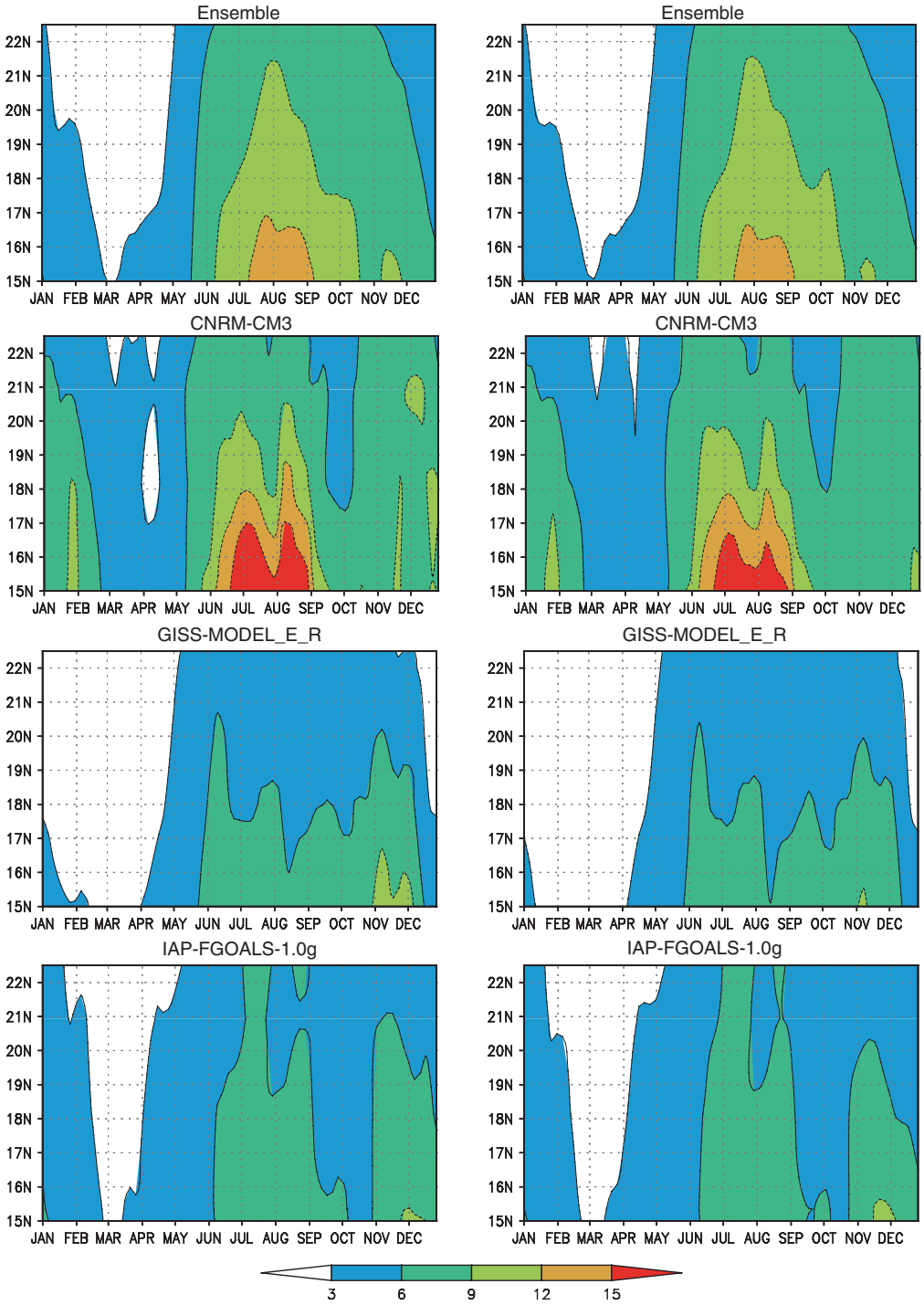

Figure 16a. The same as in Figure 9(c) and (d), but for the model simulations. The left line denotes the location at 130 °E and the right line denotes the partial zonal average between 125° and 140 °E. This figure is available in colour online at www.interscience.wiley.com/ijoc

coincidentally that the first wind onset propagates from north to south whereas the second wind onset propagates from south to north. The strong cross-equator flows have reached the WNP and the WPSH retreats eastward notably from Phase 1 to Phase 2. Both variations of circulation play key roles in triggering the first wind onset. At the same time, the WNP is an important region where the cross-equator flows encounter the easterly flows. As both flows are strong enough, and the ridge of WPSH turns to southwest–northeast direction to control WNP, the stalemate is inevitable to lead to the stable state before the second onset. Meanwhile, the intense moisture convergence is located in the SCS and the low latitude of WNP is consistent with the heavy rainbelts. With the strengthening of cross-equator flows and the sudden jumping of WPSH ridge, the monsoon trough develops in the WNP and then induces the second wind onset. The variations of OLR and rainfall are not as synchronous as the local twice wind onsets and have a difference of 5° latitude to the north over the WNP. Both the OLR and

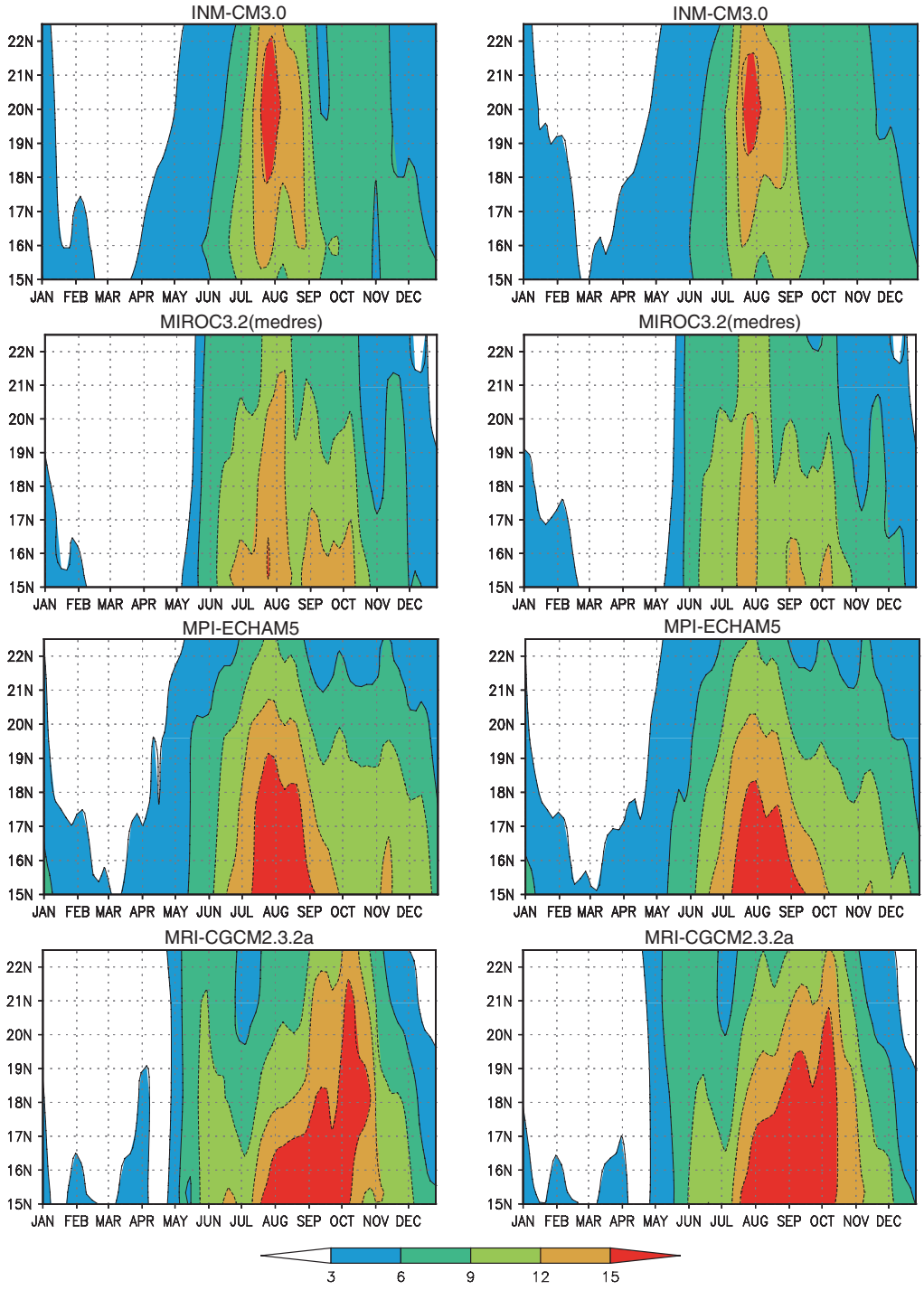

Figure 16. (*Continued*).

the rainfall show double peaks near the dates of twice wind onsets. It suggests that the impact of monsoon wind direction is not local and can result in a similar pattern in the OLR and rainfall in the northern neighbouring region.

As an independent subsystem, the WNPSM is quite different from that of the subtropical East Asian monsoon, but there are close relationships and interactions between them (Chen *et al*., 1991; Chen *et al*., 2006; He *et al*., 2007). According to the studies of Chen *et al*. (2000), the pre-flood rainy season reaches the peak after the onset of tropical monsoon, therefore the first wind onset of WNPSM is accompanied by the commencement of rainy season over South China. This may suggest that it is a sign to trigger the rainy season of subtropical monsoon. On the other hand, He *et al*. (2007) pointed out that the onset of subtropical monsoon in mid-March is in favour of the tropical summon monsoon breakout, and that it may also contribute to the wind onset of WNPSM. And during Phase 2 after the first wind onset, the WNP is covered with southeasterly, which bring a lot of moisture to South China and result in the rainy season (Liang *et al*., 2007). The southwesterly over WNP in Phase 3

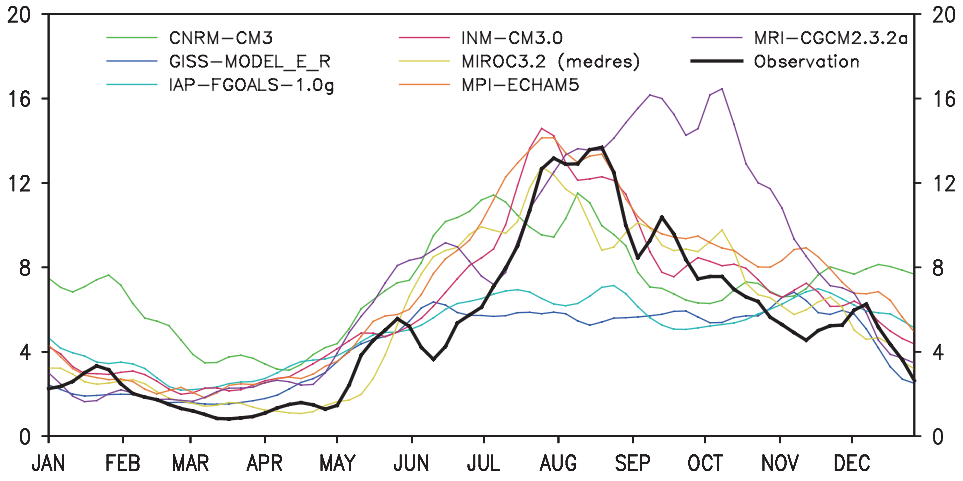

Figure 17. Seasonal variations of area-averaged surface precipitation (mm/day) of the observation and model simulations in domain of 15°–22.5 °N, 125°–140 °E. This figure is available in colour online at www.interscience.wiley.com/ijoc

after the second wind onset suggests that the moisture from South Asia plays an important role in the rainy season of WNP; therefore, both the subtropical monsoon and the WNPSM are important components for the Asian monsoon, and further studies of the WNPSM are propitious to investigate the relationships and interactions between them.

For AGCMs to be useful for monsoon studies, it is essential that the main features of the summer monsoon should be simulated with reasonable accuracy. However, we evaluate the overall performance of recent AGCMs of the IPCC AR4 in simulating the climatological variations of monsoon over the WNP, particularly focusing on its particular feature of twice wind onsets, and describe the differences among models by intercomparing their simulations. Unfortunately, most of models, including the multi-models ensemble mean, can not reproduce the twice wind onsets over the WNP reasonably well. MPI-ECHAM5 [Figure 14(g)] captures part of a similar pattern. But the dates of onsets are not coincident with those observed. Moreover, none of the models captures the observed migration of monsoon trough over the WNP. That may be one factor for the poor simulation of the dates of the second wind onset. The regional structures of the climatological mean precipitation simulated by individual models differ substantially from those observed. None of the model simulations shows the general spatial pattern similar to the corresponding observations. That may be related to the poor simulations of the variations of wind directions as the twice wind onsets would influence the northern neighbouring regions. Moreover, the shortcomings in simulated precipitation may relate to the poor simulations of OLR as the OLR is an important factor that affects summer rainfall (Li and Zhang, 2008).

The area with twice wind onsets is a key region for monsoon and tropical cyclone (Nitta 1987; Murakami and Matsumoto 1994). Although there are still notable deficiencies for AGCMs in simulating the twice wind onsets of monsoon and corresponding rainfall over the WNP, we believe that the results obtained in this study are meaningful and significant for the monsoon research and model improvement. As the realistic simulations of monsoon variability in AMIP models are dependent on their abilities to reproduce the monsoon rainfall in the WNP (Gadgil and Sajani, 1998), the twice wind onsets may provide a signal on the peculiar sudden change of wind direction and circulation, which would be helpful for further research to improve the models. It is well known that the tropical intraseasonal variability, especially the fidelity of Majjen-Julian Oscillation (MJO), plays important role to significant affect a wide range of tropical weather such as the onset and breaks of the Asian summer monsoon (Yasunari, 1979; Wheeler and McBrie, 2005; Zhou and Chan 2005). However, the current GCMs still have significant problems and display a wide range of shortcoming in simulating the tropical intraseasonal variability (Slingo *et al*,. 1996; Lin *et al*., 2006). Those shortcomings may also affect the twice wind onset of WNP. Based on the complicated synoptic mechanism over WNP, it could be stated that the large biases in the AMIP model in simulating the twice wind onset of the WNPSM are still uncertain, as they may be related to many factors. Besides, the weak simulations of the annual precipitation over the WNP are also shown in most of the newest generation of coupled climate system models (Dai, 2006). Thus, the physical mechanism of the twice wind onset should be focused on in future studies, which will contribute to the improvement of the climate model.

Acknowledgements

We acknowledge the international modelling groups for providing their data for analysis, the Program for Climate Model Diagnosis and Intercomparison (PCMDI) for collecting and archiving the model data, the JSC/CLIVAR Working Group on Coupled Modelling (WGCM) and their Coupled Model Intercomparison Project (CMIP) and Climate Simulation Panel for organizing the model data

analysis activity, and the IPCC WG1 TSU for technical support. The IPCC Data Archive at Lawrence Livermore National Laboratory is supported by the Office of Science, US Department of Energy. This work was jointly supported by the 973 Program (2006CB403600) and the National Natural Science Foundation of China (40221503, 40523001).

References

Akasaka I, Morishima W, Mikami T. 2007. Seasonal march and its spatial difference of rainfall in the Philippines. *International Journal of Climatology* **27**: 715–725.

Boyle JS. 1998. Intercomparison of interannual variability of the global 200-hPa circulation for AMIP simulations. *Journal of Climate* **11**: 2505–2529.

Chan JCL, Zhou W. 2005. PDO, ENSO and the summer monsoon rainfall over South China. *Geophysical Research Letter* **32**: L08810.

Chen J, Huang R. 2006. The Comparison of climatological characteristics among Asian and Australian monsoon subsystems. Part I. The wind structure of summer monsoon. *Chinese Journal of Atmospheric Science* **30**: 1091–1102.

Chen L, Zhu Q, Luo H, He J. 1991. *Eastern Asia monsoon*. China Meteorology Press: Beijing; 362pp.

Chen L, Li W, Zhao P, Tao S. 2000. On the process of summer monsoon onset over East Asia. *Climate and Environmental Research* **5**: 345–355.

Chen L, Gao H, He J, Tao S, Jin Z. 2004. Zonal propagation of kinetic energy and convection in the South China Sea and Indian monsoon regions in boreal summer. *Science in China Series D* **34**: 1076–1084.

Chen L, Zhang B, Zhang Y. 2006. Progress in research on the East Asian Monsoon. *Journal of Applied Meteorological Science* **17**: 711–724.

Dai AG. 2006. Precipitation characteristics in eighteen coupled climate models. *Journal of Climate* **19**: 4605–4630.

Gadgil S, Sajani S. 1998. Monsoon precipitation in the AMIP runs. *Climate Dynamics* **14**: 659–689.

Gates WL, *et al*. 1999. An overview of the results of the atmospheric model intercomparison project (AMIP1). *Bulletin of the American Meteorological Society* **80**: 29–55.

He J, Qi L, Wei J, Chi Y. 2007. Reinvestigations on the East Asian subtropical monsoon and tropical monsoon. *Chinese Journal of Atmospheric Science* **31**: 1258–1265.

Holland GJ. 1986. Interannual variability of the Australian summer. monsoon at Darwin: 1952–82. *Monthly Weather Review* **114**: 594–604.

Hsu HH, Terng CT, Chen CT. 1999. Evolution of large-scale circulation and heating during the first transition of Asian Summer Monsoon. *Journal of Climate* **12**: 793–810.

Kalnay E. 1996. The NCEP/NCAR 40-Year Reanalysis Project. *Bulletin of the American Meteorological Society* **77**: 437–471. Coauthors.

Kang IS, *et al*. 2002a. Intercomparison of the GCM simulated anomalies associated with the 1997-98 El Nino. *Journal of Climate* **15**: 2791–2805.

Kang IS, *et al*. 2002b. Intercomparison of the climatological variations of Asian summer monsoon rainfall simulated by 10 GCM's. *Climate Dynamic* **19**: 383–395.

Krishnamurthy V, Shukla J. 2000. Intraseasonal and interannual variability of rainfall over India. *Journal of Climate* **13**: 4366–4377.

Lau KM, Yang S. 1997. Climatology and interannual variability of the Southeast Asian summer monsoon. *Advance Atmospheric Science* **14**: 141–162.

Li CY, Wu J. 2000. On the onset of the South China Sea summer monsoon in 1998. *Advance Atmospheric Science* **17**: 193–204.

Li J, Zeng Q. 2000. Significance of the normalized seasonality of wind field and its rationality for characterizing the monsoon. *Science in China Series D* **30**: 331–336.

Li J, Zhang L. 2008. Wind onset and withdrawal of Asian summer monsoon and their simulated performance in AMIP models. *Climate Dynamics*. **DOI**: 10.1007/s00382-008-0465-8.

Li JP, Chou JF. 1998. Dynamical analysis on splitting of subtropical high-pressure zone – Geostrophic effect. *Chinese Science Bulletin* **43**: 1285–1289.

Liang P, Tang X, He J, Chen LX. 2007. An East Asian sub-tropic summer monsoon index defined by moisture transport. *Journal of Tropical Meteorology* **23**: 467–473 (in Chinese).

Liang XZ, Wang WC, Samel AN. 2001. Biases in AMIP model simulations of the east China monsoon system. *Climate. Dynamics* **17**: 291–304.

Liebmann B, Smith CA. 1996. Description of a complete (interpolated) outgoing longwave radiation dataset. *Bulletin of the American Meteorological Society* **77**: 1275–1277.

Lin JL, *et al*. 2006. Tropical intraseasonal variability in 14 IPCC AR4 climate models. Part I: Convective signals. *Journal of Climate* **19**: 2665–2690.

Lu E, Chang JCL. 1999. A unified monsoon index for south China. *Journal of Climate* **12**: 2375–2385.

Matsumoto J. 1992. The seasonal changes in Asian and Australian monsoon regions. *Journal of Meteorological Society Japan* **70**: 257–273.

Matsumoto J. 1997. Seasonal transition of summer rainy season over Indochina and adjacent monsoon region. *Advance Atmospheric Science* **14**: 231–245.

Murakami T, Wang B, Lyons SW. 1992. Contrasts between summer monsoons over the Bay of Bengal and the eastern North Pacific. *Journal of Meteorological Society Japan* **70**: 191–210.

Murakami T, Matsumoto J. 1994. Summer monsoon over the Asian Continent and western north Pacific. *Journal of Meteorological Society Japan* **72**: 719–745.

Ninomiya K, Murakami T. 1987. The early summer rainy season (Baiu) over Japan. In: *Monsoon Meteorology*, Chang CP, Krishramurti TN (eds). Oxford University Press: Oxford, 93–121.

Nitta T. 1987. Convective activities in the tropical western Pacific and their impact on the Northern Hemisphere summer circulation. *Journal of Meteorological Society Japan* **65**: 373–390.

Slingo JM, *et al*. 1996. Intraseasonal oscillations in 15 atmospheric general circulation models: results from an AMIP diagnostic subproject. *Climate. Dynamics* **12**: 325–357.

Soman MK, Slingo JM. 1997. Sensitivity of Asian summer monsoon to aspects of sea surface temperature anomalies in the tropical Pacific Ocean. *Quarterly Journal of Royal Meteorological Society* **123**: 309–336.

Sperber JM, Slingo JM, Annamalai H. 2000. Predictability and the relationship between subseasonal and interannual variability during the Asian summer monsoon. *Quarterly Journal of Royal Meteorological Society* **126**: 2545–2574.

Sperber KR, Palmer TN. 1996. Interannual tropical rainfall variability in general circulation model simulations associated with the Atmospheric Model Intercomparison Project. *Journal of Climate* **9**: 2727–2750.

Tao SY, Chen L. 1987. A review of recent research on East summer monsoon in China. In: *Monsoon Meteorology*, Chang CP, Krishramurti TN (eds). Oxford University Press: Oxford, 60–92.

Ueda H, Yasunari T, Kawamura R. 1995. Abrupt seasonal change of large-scale convective activity over the western Pacific in the northern summer. *Journal of Meteorological Society Japan* **73**: 795–809.

Ueda H, Yasunari T. 1996. Maturing process of summer monsoon over the western North Pacific – A coupled Ocean/Atmosphere system. *Journal of Meteorological Society Japan* **74**: 493–508.

Ueda H. 2005. Air-sea coupled process involved in stepwise seasonal evolution of the Asian summer monsoon. *Geographical Review of Japan* **86**: 825–841.

Wang B. 1994. Climatic regimes of tropical convection and rainfall. *Journal of Climate* **7**: 1109–1118.

Wang B, Wu R, Lukas R. 1999. Roles of the western North Pacific wind variation in thermocline adjustment and ENSO phase transition. *Journal of Meteorological Society Japan* **77**: 1–16.

Wang B, Wu R, Fu X. 2000. Pacific-East Asia teleconnection: How does ENSO affect East Asian climate?. *Journal of Climate* **13**: 1517–1536.

Wang B, Wu R, Lau KM. 2001. Interannual variability of Asian summer monsoon: contrast between the Indian and western North Pacific summer monsoon. *Journal of Climate* **14**: 4073–4090.

Wang B, Lin Ho. 2002. Rainy season of the Asian-Pacific summer monsoon. *Journal of Climate* **15**: 386–398.

Wang B, Lin Ho, Zhang YS, Lu MM. 2004. Definition of South China Sea monsoon onset and commencement of the East Asia summer monsoon. *Journal of Climate* **17**: 699–710.

Webster PJ, Magana VO, Palmer TN, Shukla J, Tomas RA, Yanai M, Yasunari T. 1998. Monsoons: Processes, predictability, and the

prospects for prediction. *Journal of Geophysical Research* **103**: 14,451–14,510.
Wheeler M, McBride JL. 2005. Australian-Indonesian monsoon. In: *Intraseasonal Variability in the Atmosphere-Ocean Climate System,*Lau KM, Waliser DE (eds). Springer Praxis: 125–173.
Wu R, Wang B. 2000. Interannual variability of summer monsoon onset over the Western North Pacific and the underlying processes. *Journal of Climate* **13**: 2483–2501.
Wu R, Wang B. 2001. Multi-stage onset of summer monsoon over the western North Pacific. *Climate Dynamics* **17**: 277–289.
Xie P, Arkin PA. 1997. Global precipitation: A 17-year monthly analysis base on gauge observations, satellite estimates and numerical model output. *Bulletin of the American Meteorological Society* **78**: 2539–2558.
Yanai M, Tomita T. 1998. Seasonal and international variability of atmospheric heat sources and moisture sinks as determined from NCEP-NCAR reanalysis. *Journal of Climate* **11**: 463–482.
Yasunari T. 1979. Cloudiness fluctuations associated with the Northern Hemisphere summer monsoon. *Journal of Meteorological Society Japan* **57**: 227–242.
Zhan R, Li J, He J, Li Q. 2008. A case study of double ridges of subtropical high over the western north Pacific: The role in the 1998 second Mei-yu over the Yangtze River valley. *Journal of Meteorological Society Japan* **86**: 167–181.
Zhang L, Li J. 2008. Seasonal Rotation Features of Wind Vectors and Application to Evaluate Monsoon Simulations in AMIP Models. *Climate Dynamics* **31**: 417–432., DOI:10.1007/s00382-007-0327-9.
Zhang XZ, Li JL, Ding YH, Yan JY. 2001. A study of circulation characteristics and index of South China Sea summer monsoon. *Acta Meteorological Sinica* **15**: 450–464.
Zhang YS, Li T, Wang B, Wu GX. 2002. Onset of the summer monsoon over the Indochina Peninsula: Climatology and interannual variations. *Journal of Climate* **15**: 3206–3221.
Zhou W, Chan JCL. 2005. Intraseasonal oscillations and the South China Sea summer monsoon onset. *International Journal of C1imatology* **25**: 1585–1609.
Zhou W, Chan JCL. 2007. ENSO and South China Sea summer monsoon onset. *International Journal of Climatology* **27**: 157–167.
Zhu Q, He J. 1985. On features of the upper circulation in the establishment of Asian monsoon in 1979 and its medium-range oscillation. *Journal of Tropical Meteorology* **2**: 9–18.
Zhu QG, He J, Wang P. 1986. A study of circulation differences between East-Asian and Indian summer monsoons with their interactions. *Advance Atmospheric Science* **3**: 466–477.

